

SIMULATION OF SOIL TEMPERATURE UNDER MAIZE: AN INTER-COMPARISON AMONG 33 MAIZE MODELS

Bruce A. Kimball^a, Kelly R. Thorp^a, Kenneth J. Boote^b, Claudio Stockle^c, Andrew E. Suyker^d, Steven R. Evett^e, David K. Brauer^e, Gwen G. Coyle^e, Karen S. Copeland^e, Gary W. Marek^e, Paul D. Colaizzi^e, Marco Acutis^f, Sotirios Archontoulis^g, Faye Babacar^h, Zoltán Barcza^{ij}, Bruno Basso^k, Patrick Bertuzzi^l, Massimiliano De Antoni Migliorati^m, Benjamin Dumontⁿ, JeanLouis Durando, Nandor Fodor^{j,p}, Thomas Gaiser^q, Sebastian Gayler^r, Robert Grant^s, Kaiyu Guan^t, Gerrit Hoogenboom^b, Qianjing Jiang^u, Soo-Hyung Kim^v, Isaya Kisekka^w, Jon Lizaso^x, Alessia Perego^f, Bin Peng^t, Eckart Priesack^y, Zhiming Qi^u, Vakhtang Shelia^b, Amit Kumar Srivastava^{q,z}, Dennis Timlin^{aa}, Heidi Webber^z, Tobias Weber^b, Karina Williams^{ac,ad}, Michelle Viswanathan^r, Wang Zhou^t

- a* U.S. Arid-Land Agricultural Research Center, USDA-ARS, Maricopa, AZ, 85138
b University of Florida, Agricultural and Biological Engineering, Frazier Rogers Hall, Gainesville, Florida, 32611-0570, USA
c Biological Systems Engineering, Washington State University, 1935 E. Grimes Way, PO Box 646120, Washington State University, Pullman, WA, 99164-6120
d School of Natural Resources, University of Nebraska-Lincoln, Lincoln, Nebraska, USA
e Conservation and Production Research Laboratory, USDA-ARS, Bushland, Texas, USA
f Department of Agricultural and Environmental Sciences, University of Milan, via Celoria 2 – 20133, Milan, Italy
g Iowa State University, Department of Agronomy, Ames, Iowa, 50010
h Université du Sine Saloum El Hadj Ibrahima NASS, 55 Kaolack, Senegal
i ELTE Eötvös Loránd University, Department of Meteorology, H-1117, Budapest, Hungary
j Czech University of Life Sciences Prague, Faculty of Forestry and Wood Sciences, 165 21, Prague, Czech Republic
k Michigan State University, Dept. Geological Sciences and W.K. Kellogg Biological Station, 288 Farm Ln, 307 Natural Science Bldg., East Lansing, MI, 48824
l US1116 AgroClim, INRAE centre de recherche Provence-Alpes-Côte d'Azur, 228, route de l'Aérodrome, CS 40 509, Domaine Saint Paul, Site Agroparc, 84914 Avignon Cedex 9, France
m Queensland Department of Environment, Science, and Innovation, Queensland, Australia
n ULiège-GxABT, University of Liège - Gembloux Agro-Bio Tech, TERRA Teaching and research centre, Plant Science Axis / Crop Science Lab., B-5030, Gembloux, Belgium
o Unité de Recherches Pluridisciplinaire Prairies et Plantes Fourragères, INRAE, 86 600, Lusignan, France
p Agricultural Institute, Centre for Agricultural Research, H-2462 Martonvásár, Brunszvik u. 2., Hungary
q Institute of Crop Science and Resource Conservation, University of Bonn, Katzenburgweg 5, D-53115, Bonn, Germany
r Universität Hohenheim, Institute of Soil Science and Land Evaluation, Biogeophysics, Emil-Wolff-Str. 2 7, D-70593, Stuttgart, Germany
s Department of Renewable Resources, University of Alberta, Edmonton, Alberta, Canada, T6G 2E3
t College of Agricultural, Consumer and Environmental Sciences (ACES), University of Illinois at Urbana-Champaign, Urbana, Illinois, 61801, USA
u Department of Bioresource Engineering, Macdonald Campus, McGill University, 1-024 Macdonald-Steward Hall, Sanite-Anne-de-Bellevue, QC, Canada, H9 × 3V9
v School of Environmental and Forest Sciences, University of Washington, WA, 98195
w Agricultural Water Management and Irrigation Engineering; University of California Davis; Departments of Land, Air, and Water Resources and of Biological and Agricultural Engineering; One Shields Avenue; PES 1110; Davis, CA, 95616-5270, USA
x Technical University of Madrid (UPM), Dept. Producción Agraria-CEIGRAM, Ciudad Universitaria, 28040, Madrid, Spain
y Helmholtz Center Munich, Institute of Biochemical Plant Pathology, Ingolstaedter Landstr. 1 85764, Neuherberg, Germany
z Leibniz Centre for Agricultural Landscape Research (ZALF), Muencheberg, 15374, Germany
aa Adaptive Cropping Systems Laboratory, USDA-ARS, Beltsville, MD
ab Soil Science Section, University of Kassel, Nordbahnhofstraße 1a, 37213, Witzenhausen, Germany
ac Hadley Centre, FitzRoy, Road Exeter Devon EX1 3PB, United Kingdom
ad Global Systems Institute, University of Exeter, North Park Road, Exeter, EX4 4QE, UK

KEYWORDS: Soil temperature, Crop models, Simulation, Prediction, Maize, Soil heat flux

ABSTRACT

Accurate simulation of soil temperature can help improve the accuracy of crop growth models by improving the predictions of soil processes like seed germination, decomposition, nitrification, evaporation, and carbon sequestration. To assess how well such models can simulate soil temperature, herein we present results of an inter-comparison study of 33 maize (*Zea mays* L.) growth models. Among the 33 models, four of the modeling groups contributed results using differing algorithms or “flavors” to simulate evapotranspiration within the same overall model family. The study used comprehensive datasets from two sites - Mead, Nebraska, USA and Bushland, Texas, USA wherein soil temperature was measured continually at several depths. The range of simulated soil temperatures was large (about 10-15 °C) from the coolest to warmest models across whole growing seasons from bare soil to full canopy and at both shallow and deeper depths. Within model families, there were no significant differences among their simulations of soil temperature due to their differing evapotranspiration method “flavors”, so root-mean-square-errors (RMSE) were averaged within families, which reduced the number of soil temperature model families to 13. The model family RMSEs averaged over all 20 treatment-years and 2 depths ranged from about 1.5 to 5.1 °C. The six models with the lowest RMSEs were APSIM, ecosys, JULES, Expert-N, SLFT, and MaizSim. Five of these best models used a numerical iterative approach to simulate soil temperature, which entailed using an energy balance on each soil layer. whereby the change in heat storage during a time step equals the difference between the heat flow into and that out of the layer. Further improvements in the best models for simulating soil temperature might be possible with the incorporation of more recently improved routines for simulating soil thermal conductivity than the older routines now in use by the models.

1. Introduction

1.1. BACKGROUND FOR INTER-COMPARING CROP GROWTH MODELS IN THEIR ABILITY TO SIMULATE SOIL TEMPERATURE (ST)

Soil is a huge reservoir for heat storage in the soil-plant-atmosphere system. Some of the solar and sensible energy received each day is conducted into the soil reservoir, and during the night some is conducted back to the soil surface where it heats the air or radiates out to a cold sky or plant canopy. The amount of heat in the soil reservoir determines the soil temperature (ST), which in turn affects soil processes and plant growth. In the case of annual plants, such as maize (*Zea mays* L.), ST must be warm enough in the spring for seeds to germinate, and then the length of time to attain emergence is strongly governed by ST. For other crops such as winter wheat (*Triticum aestivum* L.) the crown of the plant is at or below the soil surface for many months until the ST warms enough in the spring for the plants to begin to grow. Of course, root respiration and other root processes affect plant growth all growing season long. Similarly, soil microbial processes also are affected by ST, including decomposition and nitrification, so the nutrient supply to plant roots and subsequent plant growth and yield are also affected. The soil water balance is also affected by near surface and surface ST because evaporation from the soil surface, dewfall, and frost accumulation are all functions of temperature near and at the surface. Therefore, it behooves crop growth models to simulate ST well in order to properly simulate crop growth, yield, water use, and soil processes.

Under the umbrella of AgMIP (agricultural model inter-comparison and improvement project), we recently conducted an inter-comparison among 41 maize growth models in their ability to simulate evapotranspiration (ET; Kimball et al., 2023). During that exercise, some of the modelers also simulated STs, and herein we present the results of this inter-comparison among 33 models in their ability to simulate STs compared with measured field data. Similar to the ET paper, our primary objective is to identify those models and approaches that are most accurate for simulating ST.

Few inter-comparisons in the ability of crop growth models to simulate ST have been reported before. Two such model inter-comparisons were done on grassland that included a few models that could also handle annual crops like maize. Biome-BGCMuSo was one of two models compared by Sándor et al. (2016) and is also included herein. It achieved an average relative root mean square error (RRMSE) of 41 %, but the authors noted that improvement is needed. Another nine-model grassland inter-comparison included Biome-BGCMuSo, ARMOSA, and STICS that are also compared herein (Sandor et al., 2017). RRMSEs ranged from 15 to 290 %, but the tabulated results were all anonymous, so it is not possible to ascertain which models and approaches were best for simulating ST. A third inter-comparison was done under maize by Archontoulis et al. (2014) using APSIM with two “flavors” of ST routines. One was the “default” based on Williams et al. (1984) and the other was an “optional” routine that used a numerical soil-layered energy balance routine from Campbell (1985). Both simulated ST well (RRMSE < 17 %) at shallow depths (0-20 cm), but at deeper depths, the optional model did much better (RRMSE = 9.3 %) than the default model (RRMSE = 26 %). As will

be seen, both of these approaches have been used by several models and similar results were obtained.

1.2. BASIC SOIL TEMPERATURE PHYSICS AND LITERATURE REVIEW

As written in many soil physics texts (e.g., Campbell, 1977), the theory of the physics of heat flow through a slab or layer of uniform material was established centuries ago by Fourier, whose “law” can be written as:

$$G = \kappa(\Delta T / \Delta z) \quad (1)$$

Where G is the soil heat flux (W/m^2), ΔT is the temperature difference across the material ($^{\circ}C$), Δz is the length of the path of heat flow (m), and κ is the thermal conductivity ($W m^{-1} ^{\circ}C^{-1}$). Values of κ vary from about $0.22 W m^{-1} ^{\circ}C^{-1}$ for dry clay to about $2.2 W m^{-1} ^{\circ}C^{-1}$ for wet sand (van Wijk and De Vries, 1963). A slab of material with more heat flowing in than out will increase in temperature with time, t (seconds or other useful time units). The rate of temperature increase is proportional to the heat flux difference, ΔG , between the heat flow in minus the heat flow out and inversely proportional to the slab thickness as shown in Eq. (2).

$$\Delta T / \Delta t = (1/C)(\Delta G / \Delta z) \quad (2)$$

where C is the volumetric heat capacity ($J m^{-3} ^{\circ}C^{-1}$). Values of C vary from about $1.3 MJ m^{-3} ^{\circ}C^{-1}$ in dry soil to $2.9 MJ m^{-3} ^{\circ}C^{-1}$ in wet soil for both clay and sand (DeVries, 1963). Of course, neither κ nor C are constant through the whole profile of a field soil because they vary with particle constituents, bulk density (ρ_b), water content (θ), and soil temperature. Yet, Eqs. (1) and 2 enable an energy balance (i.e. change in heat storage equals G_{in} minus G_{out} .) to be written for each layer within a soil profile where each layer would have near constant κ and C . Then numerical methods can be used to solve the resultant set of simultaneous equations for the temperature of each layer, and as will be discussed, several models used this approach to simulate ST (Table S1).

However, if the temperature at the soil surface, T_o , follows a sine wave (annual or daily) such as:

$$T_o = T_{avg} + A \sin(\omega t + \varphi) \quad (3)$$

Where T_{avg} is the average temperature ($^{\circ}C$) during a cycle, A is the amplitude of the wave ($^{\circ}C$), φ is the phase of the wave at the soil surface (radians), and ω is the angular velocity (radians per second or per day or per year as appropriate); then if κ and C are constant with depth and time, the temperature at any given depth and time can be calculated from (i.e., Campbell, 1977):

$$T(z, t) = T_{avg} + A \exp(-z / D) \sin[\omega t + \varphi - (z / D)] \quad (4)$$

$$\text{where } D = (2\kappa C^{-1} \omega^{-1})^{0.5} \quad (5)$$

is the so-called damping depth (m) at which the amplitude of A is attenuated exponentially by $1/e$. Eq. (4) is a sine wave that is damped with depth and lagged with time into the soil. The graph on the cover and Figure 2.6 (attributed to C. Tongyai) of Campbell (1977) shows it nicely. However, as already mentioned, neither κ nor C are generally constant with depth and time in soil. Further, while annual temperatures tend to vary sinusoidally, T_o is also affected by varying weather patterns,

amount of crop leaf area, whether the crop is water-stressed, etc. Typical diurnal temperature patterns follow a sine curve from dawn until mid-afternoon but after that, they follow an exponential decay until dawn the next morning (Parton and Logan, 1981; Kimball and Bellamy, 1986), and of course, they too are altered by changing weather and crop characteristics. Nevertheless, Eq. (4) enables an estimate of the ST at every depth and time to be quickly and analytically calculated. Therefore, as will be discussed, several models follow this alternative analytical approach to simulate ST (Table S1).

1.3. SIMULATING SOIL HEAT CAPACITY

Whether using analytical Eq. (4) or using numerical Eq. (2) applied to all individual layers, representative values of thermal conductivity and heat capacity (or just damping depth) are needed in order to obtain accurate simulations of soil temperature. De Vries (1963) presented “classic” theoretical equations for calculating both, as well as typical values, and many of the models use his methodology and values (Table S1). His equation for heat capacity is based on well-defined parameters, is used by almost all the models, and apparently no one has published improved alternatives. It is the sum of the specific heats of individual components of soil [i.e., mineral particles, organic matter particles, and water (air is insignificant)], each multiplied by its volume fraction.

Thus, heat capacity is subject to variability in bulk density and water content, both of which can change with depth and time.

1.4. SIMULATING SOIL THERMAL CONDUCTIVITY

Similar to heat capacity, De Vries’s (1963) “classic” thermal conductivity equation varies with the thermal conductivities of the individual components of soil and their volume fractions. However, it’s more complicated because it also varies with the shape of the mineral and organic particles, so therefore, his equation also has particle shape factors. His equation also addresses the degree to which water coats the particles and provides paths between them. Of course, liquid water movement can also carry heat, which is important when there are precipitation or irrigation events, but these events are transient. However, if all this isn’t complicated enough, with temperature gradients in the soil, water vapor can diffuse from higher to lower temperature areas in the soil, thereby carrying latent heat and increasing the thermal conductivity of the soil. However, between day and night, temperature gradients reverse direction, so on a daily time scale (as opposed to hourly), latent heat transport is less important. However, even on sub-daily time scales, Kimball et al. (1976) concluded that thermal and isothermal vapor fluxes exactly cancelled during the day and were insignificant at night in a field experiment with bare clay loam soil over several seasons of a year. However, they also found their best fit of De Vries’s (1963) model to data was obtained by changing the air shape factor to negative values, which are physically unrealistic, yet could serve as empirical coefficients. Thus, as also stated by Evett et al. (2012), the shape factors become fitting parameters.

Apparently, none of the 33 models included in this inter-comparison included vapor movement, because no references about vapor movement are cited by the modelers (Table S1).

Since DeVries (1963), there are a few reports of development of more recent equations to simulate soil thermal conductivity along with comparison measurements. McInnes et al. (1986) presented an equation relating thermal conductivity to soil water content relative to saturation which had five fitting parameters. Hoffmann et al. (1993) developed empirical equations for each of the McInnes et al. parameters relating A to fractions of quartz and of other minerals, B to bulk density and water content, C to clay content, D to bulk density squared, and E is a constant (4.0). The McInnes-Hoffmann equation is used in the SALUS model (Table S1). More recently Evett et al. (2012) fitted their soil thermal conductivity measurements to the McInnes equation. Figure 6 in Evett et al. (2012) shows that soil thermal conductivity is weakly related to bulk density and almost linearly related to soil moisture. However, their soil moisture range only went from 0.05 to 0.22, and their Figure 6 does not show the precipitous drop in thermal conductivity below 0.05 observed by, for example, De Vries (1963), Campbell et al. (1994), and Côte and Konrad (2005).

Campbell et al. (1994) studied the effect of high temperatures (forest fire) on soil thermal conductivity, but they also included lower temperatures of 30 °C and 50 °C in their experiments and modeling. They modified the thermal conductivity theory of De Vries (1963) somewhat and obtained quite good agreement between predicted and measured values for seven soils and peat moss across a range of bulk density and soil water content for the 30 °C and 50 °C temperatures.

Côte and Konrad (2005) following Johansen (1975) used a more empirical approach. They normalized the thermal conductivity versus water content curve of soil with the oven-dry thermal conductivity at the dry end and with the saturated thermal conductivity at the wet end. The resultant normalized curves for a variety of soils and other porous material coalesced into a much smaller band. The curvature varied somewhat with texture, but after testing many materials they provided curvature shape values for coarse sands and gravels, for medium and fine sands, and for silty and clayey soils. They also provide methods to calculate the oven-dry and water-saturated conductivities. However, the experimental data in De Vries (1963), Campbell et al. (1994), and even in Côte and Konrad (2005) follow a sigmoidal curve with little change from a minimum thermal conductivity at zero water content to a threshold at about 0.02-0.05 m³/m³ where apparently the water films around particles become continuous, and then there is an abrupt rise in conductivity following a more parabolic curve. Lu et al. (2007) recognized the threshold, and they developed a new model that again normalizes the conductivity at zero and saturated water contents but accounts for the threshold. Their model worked well over the entire water content range, and they also presented a simpler equation to compute the conductivity at zero water. However, they only worked at 20 °C. Nevertheless, their RMSEs of about 0.08 W m⁻¹ K⁻¹ were only slightly larger than those of the more complicated model of Campbell et al. (1994) for their 30 °C curve.

More recently Mahdavi et al. (2016) did an inter-comparison among four similar soil thermal conductivity models that started with (I) De Vries (1963), (II) some modifications by Campbell et al. (1994) to extend De Vries (1963) to 600 °C, (III) same as II except particle shapes assumed spherical, and (IV) following Nobre and Thomson (1993) same as I with needle-shaped particles and a modified

shape factor for water. They studied four soils from coarse sand to clay loam at 28, 38, and 48 °C. The De Vries-Campbell Model III had the lowest RMSEs of about $0.22 \text{ W m}^{-1} \text{ K}^{-1}$ for coarse sand and about 0.16 for loams. However, these RMSEs are about double those reported by Campbell et al. (1994) for his model at 30 °C and those reported for the normalization model of Lu et al. (2007). Unfortunately, so far as we are aware, no one has done an inter-comparison between the De Vries-Campbell approach and the Lu et al. (2007) normalization approach. In any event, the use of these more recent models for soil thermal conductivity along with the De Vries model for heat capacity may be an avenue for further improvement of crop growth models in their ability to simulate soil temperature, whether using the numerical Eq. (2) or analytical Eq. (4).

1.5. SIMULATING DAMPING DEPTH

In the EPIC (Williams et al., 1984, 1989) and APEX (Williams et al., 2005, 2008) empirical equations based on bulk density and water content are used to simulate damping depth without separate identifiable equations for thermal conductivity or heat capacity. A similar approach is used in the DSSAT-CSM family of models (Hoogenboom et al., 2019a, b; Jones et al., 2003).

2. Materials and methods

2.1. OBSERVED DATA

2.1.1. UNIVERSITY OF NEBRASKA, MEAD, NEBRASKA, USA

As we reported in Kimball et al. (2023), data came from one irrigated field and another rainfed field within 1.6 km of each other at the University of Nebraska, Eastern Nebraska Research, Extension and Education Center near Mead, Nebraska, USA (<http://csp.unl.edu/public/>). The soils were deep silty clay loams of Yutan (fine-silty, mixed, superactive, mesic Mollic Hapludalfs), Tomek (fine, smectitic, mesic Pachic Argialbolls), Filbert (fine, smectitic, mesic Vertic Argialbolls), and Filmore (fine, smectitic, mesic Vertic Argialbolls). Both fields were strictly no-till so plant residues were not ploughed into the soil, and the soil surface was generally partially covered with prior maize/soybean crop residue, which could have affected soil heat flux early in the growing seasons. However, at the irrigated field from 2010 to 2013, conservation tillage was employed as part of a stover removal project. Both sites are part of the Ameriflux (<https://ameriflux.lbl.gov/sites>; US-Ne2 and US-Ne3) U.S. surface gas flux observation system. The eddy covariance technique was used to determine ET of maize and soybean (*Glycine max*) in alternate years (maize in 2003, 2005, 2007, 2009, 2011, 2013), as well as fluxes of sensible heat and CO₂. Thus, there were 12 treatment-years (2 water regimes x 6 years) of data. Soil water contents in the root zone were monitored continuously at four depths (0.10, 0.25, 0.5, and 1.0 m) at three and four locations in the irrigated and rainfed fields (Intensive Measurement Zones or IMZ's), respectively employing Theta probe sensors (Model ML2, Delta-T Devices, Cambridge, UK) (Suyker and Verma, 2008, 2009). Installation holes were drilled at an angle

of approximately 45° to the respective depth and the probe inserted into the bottom of the hole. Additional details can be found in Suyker and Verma (2008, 2009) and Suyker et al. (2004, 2005).

Soil temperatures were measured in one location near the eddy covariance tower using an array of soil thermistors (model YSI44004, YSI Precision™ Thermistors and Probes, Dayton, OH). They were installed horizontally in-row and between row at 0.02, 0.06, 0.08, and 0.10 m using a custom designed depth guide. Three probes at 0.20, 0.30, and 0.50 m were installed vertically between rows (total of 11 sensors). A simple half-bridge circuit was used to measure resistance of each thermistor. Hourly data were collected and then averaged to produce daily ST data to compare with simulated values from the models.

2.1.2. USDA, AGRICULTURAL RESEARCH SERVICE, CONSERVATION AND PRODUCTION RESEARCH LABORATORY, BUSHLAND, TEXAS, USA

Also, as we reported in Kimball et al. (2023), maize was grown in 2013 and 2016 at the USDA-ARS Conservation and Production Research Laboratory (<https://www.ars.usda.gov/plains-area/bushland-tx/cprl/>), Bushland, Texas (35.18° N, 102.10° W, 1170 m above MSL) on a gently sloping (<0.3 %) Pullman soil (fine, mixed, superactive, thermic Torrertic Paleustoll). Additional details and data are provided by Evett et al. (2019, 2020, 2022). Four 4.4 ha fields, approximately square in shape and adjacent to each other, each contained a large (3 m × 3 m in surface area, 2.3 m deep) precision weighing lysimeter in the center. The fields and their associated lysimeters were designated NE, SE, NW, and SW according to the inter-cardinal directions. The NE and SE lysimeters and fields were irrigated to replace 100 % of soil moisture lost by ET using subsurface drip irrigation (SDI). The NW and SW lysimeters and fields were irrigated by mid-elevation sprinkler application (MESA) using a ten-span linear-move system described by Evett et al. (2019) with the NW receiving 100 % and SW receiving 75 % of soil moisture replacement. Thus, there were 8 treatment-years of data from Bushland [(1 field of 100 % MESA + 1 field of 75 % MESA + 2 fields of 100 % SDI) × 2 years] plus the 12 treatment-years from Mead for a total of 20 treatment-years.

In the large, precision weighing lysimeters at Bushland, TX, ST was sensed every six seconds and reported as 15-minute mean values. The 15-minute data were then averaged over individual days to obtain daily ST data to compare with the simulated values from the models. Temperatures at 2- and 6-cm depths were sensed in each lysimeter using soil water and temperature sensors (model 315 L, Acclima, Inc., Meridian, Idaho) that were calibrated against standards traceable to the National Institute of Standards and Technology. Sensors were placed at two locations within the weighing lysimeter. One location was halfway between the 1st row north of the south side of the lysimeter monolith and the interrow north of that row. The other location was halfway between the 2nd row north of the south side of the lysimeter monolith and the interrow north of that row. Both sensors were 50 cm west of the east side of the lysimeter monolith. Temperatures at the 100-cm depth in each lysimeter were sensed using a calibrated copper-constantan thermocouple encased in a stainless-steel sheath (similar to model TJ36-ICIN, Omega Engineering, Norwalk, CT, USA) at a point 1 m from the wall of the lysimeter monolith.

The thermocouple sensors were installed by drilling a hole through the steel lysimeter wall at a depth 100 cm below the soil surface and drilling a 1.6-mm diameter hole horizontally into the soil monolith followed by pushing the stainless-steel sheathed thermocouple into the hole and sealing the hole in the lysimeter wall against leakage. Both the size of the soil monolith (3 m × 3 m × 2.3 m) and the distance of the thermocouple from the steel wall were design factors chosen to limit the influence of heat conduction in the steel wall on soil temperature readings (Black et al., 1968; Dugas and Bland, 1991). The stainless-steel sheath was not in direct contact with the lysimeter steel wall, and tests of the influence of temperature changes at the proximal end of the meter-long sensor on the temperature sensed by the thermocouple at the distal end of the sensor indicated negligible effect on sensed temperatures.

The soil water and temperature sensors were installed at precise depths below the soil surface in the following way. First, the lysimeter soil surface was leveled, then an 18-mm thick flat plywood form was laid on the flat surface. The form had a cut out that allowed excavation of the soil beneath while leaving the outer perimeter of the form resting on the leveled soil surface.

2.2. MODELING METHODOLOGY

2.2.1. MODEL LIST

The simulations were conducted by 13 modeling groups from around the world with 33 models completing the inter-comparison (Table 1). Details about each model are presented in supplementary Table S1. Most of the models used hourly time steps, but some used hourly and then computed daily averages. Comparisons between simulated and observed STs were done on daily average STs. As can be seen from the names (Tables 1, S1), in some cases there were several “flavors” of different simulation methods tested within the same model family that were chosen by the user at run time. The biggest example is that of the DSSAT-CSM family (Hoogenboom et al., 2019a,b; Jones et al., 2003) of the cropping system model (CSM) within which both the CSM-CERES-Maize and CSM-IXIM-Maize (hereafter simply called CERES and IXIM) modules were run. Both calculate a value called potential evapotranspiration, which was done using four methods: (1) FAO-56 (Allen et al., 1998), (2) Priestley-Taylor (1972), (3) the ASCE Standardized Reference Evapotranspiration Equation (Allen et al., 2005) for 12-cm grass (short crop), and (4) the ASCE Equation for 50-cm alfalfa (tall crop; *Medicago sativa* L.) with FAO-56 dual crop coefficients for maize (Table S1). Within these eight combinations, two E methods for calculating soil water evaporation were tested: “Ritchie” (Ritchie, 1972) and “Suleiman” (Suleiman and Ritchie, 2003, 2004). In addition, within the CERES-FAO-56 and CERES-Priestley-Taylor combinations, E was also computed using Hydrus (Simunek et al., 1998, 2008; Shelia et al., 2018), in which soil water moves based on potential gradients. Thus, there were a total of 18 (2 models × 4 ETp methods × 2 soil E methods + 2 Hydrus) DSSAT flavors. Within the DSSAT flavors, model calibrations were aimed at the best statistics [lowest RMSE, and highest D-statistic (Willmott, 1982)] for growth, grain yield, ET, and soil water variables, averaged over four ET options (two ET by two E methods) in order to minimize bias.

In addition, Expert-N had GECROS and SPASS flavors, STICS had KETP and ETP_SW flavors, and MAZSIM had daily and hourly flavors.

Table 1. List of models and their acronyms. Within the table there are 18 “flavors” of models within the DSSAT-CSM family that differ in their methodology for simulating evapotranspiration (ET). Similarly, there are two flavors each in the MAZSIM, Expert-N, and STICS model families. For details about the soil temperature simulation aspects of each, see “Supplementary Table S1: List of Models Plus Their Soil Temperature Characteristics.”

Acronym	Model Name	Reference
AMSW	APSIM-SOILWAT	Keating et al., 2003
ARMO	ARMOSA	Perego et al., 2013
BIOM	Biome-BGCMuSo 6.0.2	Hidy et al., 2016
DACT	DayCent-CABBI	Moore et al., 2020
DCAR	DSSAT CSM-CERES-Maize ASCE-Alfalfa Ritchie	DeJonge and Thorp, 2017
DCAS	DSSAT CSM-CERES-Maize ASCE-Alfalfa Suleiman	DeJonge and Thorp, 2017
DCFH	DSSAT CSM-CERES-Maize FAO-56 Hydrus	Shelia et al., 2018
DCFR	DSSAT CSM-CERES Maize FAO-56 Ritchie	Sau et al., 2004
DCFS	DSSAT CSM-CERES-Maize FAO-56 Suleiman	Sau et al., 2004
DCGR	DSSAT CSM-CERES-Maize ASCE-Grass Ritchie	DeJonge and Thorp, 2017
DCGS	DSSAT CSM-CERES-Maize ASCE-Grass Suleiman	DeJonge and Thorp, 2017
DCPH	DSSAT CSM-CERES-Maize Priestley-Taylor Hydrus	Shelia et al., 2018
DCPR	DSSAT CSM-CERES-Maize Priestley-Taylor Ritchie	Sau et al., 2004
DCPS	DSSAT CSM-CERES-Maize Priestley-Taylor Suleiman	Sau et al., 2004
DIAR	DSSAT CSM-IXIM-Maize ASCE-Alfalfa Ritchie	DeJonge and Thorp, 2017
DIAS	DSSAT CSM-IXIM-Maize ASCE-Alfalfa Suleiman	DeJonge and Thorp, 2017
DIFR	DSSAT CSM-IXIM-Maize FAO-56 Ritchie	Sau et al., 2004
DIFS	DSSAT CSM-IXIM-Maize FAO-56 Suleiman	Sau et al., 2004
DIGR	DSSAT CSM-IXIM-Maize ASCE-Grass Ritchie	DeJonge and Thorp, 2017
DIGS	DSSAT CSM-IXIM-Maize ASCE-Grass Suleiman	DeJonge and Thorp, 2017
DIPR	DSSAT CSM-IXIM-Maize Priestley-Taylor Ritchie	Sau et al., 2004
DIPS	DSSAT CSM-IXIM-Maize Priestley-Taylor Suleiman	Sau et al., 2004
ECOS	Ecosys	Grant and Flanagan, 2007
JUL	JULES	Best et al., 2011
L5SH	L5-SLIM-H	Wolf, 2012
MZD	MAZSIM Daily	Kim et al., 2012
MZH	MAZSIM Hourly	Kim et al., 2012
SLUS	SALUS	Basso and Ritchie, 2015
SLFT	SIMPLACE LINTUL5 FAO56 SLIM3 CanopyT	Wolf, 2012
STCK	STICS_KETP	Brisson et al., 2003
STSW	STICS_ETP_SW	Brisson et al., 2003
XNGM	Expert-N - GECROS	Priesack et al., 2006
XNSM	Expert-N - SPASS	Priesack et al., 2006

2.2.2. SIMULATION PROTOCOL

The study was conducted in four phases with the modelers receiving successively more information with each phase, thereby enabling progressively more model calibration with each phase. The phases were (1) “blind phase” wherein the modelers received only soils, weather, and crop management information, (2) “potential or non-stressed growth phase” wherein they received leaf area index, biomass, and grain yield for non-water-stress treatments, (3) “non-stress ET phase” wherein they received ET, soil water, and ST for non-water-stress treatments, and (4) “All phase” wherein this final phase, the modelers were provided with all LAI, biomass, grain yield, ET, soil moisture, soil temperature etc. data for all treatment-years. However, in the analysis of the ET and agronomic data, some model simulations improved with the progressive information, while a few did worse. In any event, we decided to just focus on the Phase 4 “All” data for these analyses of ST simulations.

The modelers were told to start their simulations on day-of-year 91 (DOY 91; April 1st), so there would be time for equilibration of soil moisture and ST. They were provided “initial” soil water content profiles but not initial ST profiles. By starting on DOY 91 for the Mead data, there were 21 days before planting in 2009 and more than a month for all other years. In Bushland, DOY 91 was about 6 weeks before planting. Therefore, there should have been enough time so that differences in initial soil temperatures probably were not important. The modelers were also supplied the average long-term air temperature for each site as well as the annual “amplitude”, which was actually the range between the monthly mean air temperature of the warmest month minus that of the coldest month.

2.2.3. METHODS FOR EVALUATING MODEL PERFORMANCE

Correlation coefficients (r), D statistics (Willmott, 1982), root mean squared errors between observed and simulated values (RMSE), normalized root mean squared errors (nRMSE), average differences, as well as mean squared deviations (MSD), standard bias (SB), non-unity of slopes (NU), and lack of correlations (LC) following Gauch et al. (2003), are all presented as Supplementary Statistical Data. The statistics and graphs were done for the 10- and 50-cm depths for Mead and for the 6- and 100-cm depths for Bushland. Also included are slopes and intercepts of regressions of observed on simulated data, along with corresponding graphs for all 33 models plus the median. Thus, for 33 models plus median, 20 treatment-years, and 2 depths there are a total of 1360 graphs.

Herein, we chose to present the RMSE results ($^{\circ}\text{C}$) calculated using:

$$\text{RMSE} = [n^{-1}\sum(P_i - O_i)^2]^{0.5}$$

where n = number of observations and P_i and O_i are the simulated and observed i th value pair. Although we used nRMSE for the ET analyses (Kimball et al., 2023), and although the inter-comparisons described in the Introduction used relative (RRMSE, same as normalized), we choose not to use nRMSE or RRMSE for temperature data because the values depend greatly on the temperature scale ($^{\circ}\text{C}$, $^{\circ}\text{K}$, or $^{\circ}\text{F}$). Although, RMSE shows the magnitudes of the temperature errors in degrees, which are easily understood, the RMSE does not indicate the type of error. Following Gauch et al. (2003), there are three ways that the simulated values can deviate from the observations. First, there can be a standard bias (SB) = $(\bar{P} - \bar{O})^2$, where \bar{P} is the average of the

modeled values and \bar{O} is the average of the observations. Second, there can be a non-unity of the regression slope (NU) = $(1 - b)^2 * (\Sigma(P_i - \bar{P})^2 / n)$, where b is the slope. Third, there can be a lack of correlation (LC) = $(1 - r^2) * (\Sigma(O_i - \bar{O})^2 / n)$, where r is the correlation coefficient. Following Gauch et al., $MSE = n^{-1} \Sigma(P_i - O_i)^2 = SB + NU + LC$. Therefore, we have additionally supplied stacked bar graphs of SB, NU, and LC.

3. Simulation results

3.1. OVERALL RMSE AND MSE COMPONENTS OF DAILY SOIL TEMPERATURE (ST) FOR ALL 33 MODELS AVERAGED OVER ALL 20 TREATMENT-YEARS AND TWO DEPTHS

The RMSE of daily ST for each season averaged over all 20 treatmentyears and 2 depths ranged from about 1.6 °C for Model 44 to about 5.3 °C for many of the models (Figure 1a). Further, the largest source of the error was the standard bias (SB) especially in the worst models (Figure 1b). The amount of the lack of correlation (LC) was similar in most of the models, which suggests this amount of deviation could due to scatter in the observed data and input parameters. Perusing the graphs in Supplementary Statistics and Graphs, essentially all the models with the largest RMSE in Figure 1a consistently simulated STs that were too warm. It turns out that these models mostly belonged to the DSSAT-CSM family, and the many “flavors” were not statistically different from one another in Figure 1a. Therefore, surprisingly, the many different “flavors” of ways to simulate ET within the family had little effect on simulating ST. This is likely because all the DSSAT flavors used the same “default” ST routine, which was relatively uncoupled from the ET methodology. The default routine in APSIM described earlier by Archontoulis et al. (2014) behaved similarly. The routine apparently used Eq. (4) with empirical expressions for A and D . Somewhat similarly, there were no significant differences between flavors of models within the STICS, Expert-N, and MaizSim families. Because the 18 flavors of DSSAT-CSM represented more than half of the total of 33 models, the median was heavily biased to the too warm temperatures of DSSAT-CSM (Figs. 1a,b). Therefore, because the RMSEs for all the 18 DSSAT-CSM flavors were not significantly different from one another, the RSMEs, SBs, NLs, and LCs were averaged across the DSSAT-CSM family, as well as across the STICS, Expert-N, and MaizSim families. This averaging reduced the number of curves or bars from 33 models to 13 model “families” in the following figures, although 9 of the “families” were represented by only a single model.

Figure 1. (a.) Overall Root Mean Square Errors (RMSE) of daily soil temperature simulations for the 33 models listed in Table 1 for 20 treatment-years and 2 depths. The RMSE was calculated for each of the 20 treatment-years at the 10- and 50-cm depths for Mead and at the 6- and 100-cm depths for Bushland. Then these RMSEs were averaged for the 20 treatment-years and the two depths to obtain the overall RMSEs shown in the graph, along with the corresponding standard errors indicated by the whiskers on the bars. The model numbers are those used in the evapotranspiration paper (Kimball et al., 2023) with only the best six model families identified by name in subsequent figures. (b.) Similar to (a.), but instead the mean square errors (MSE) are plotted as stacked bars following Gauch et al. (2003) to proportion the variances into standard biases (SB), non-linearity of the slopes (NL), and the lack of correlations (NC).

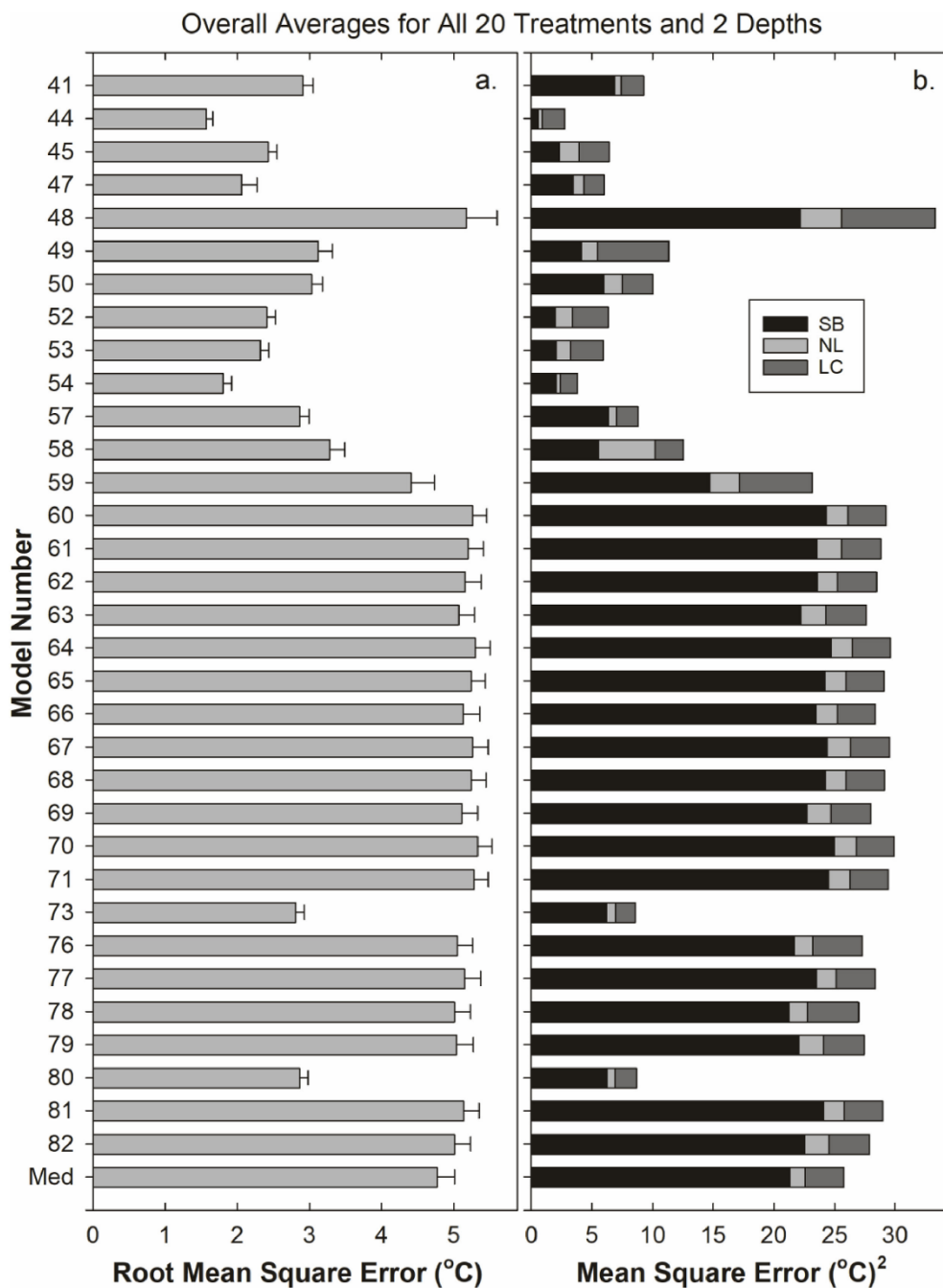
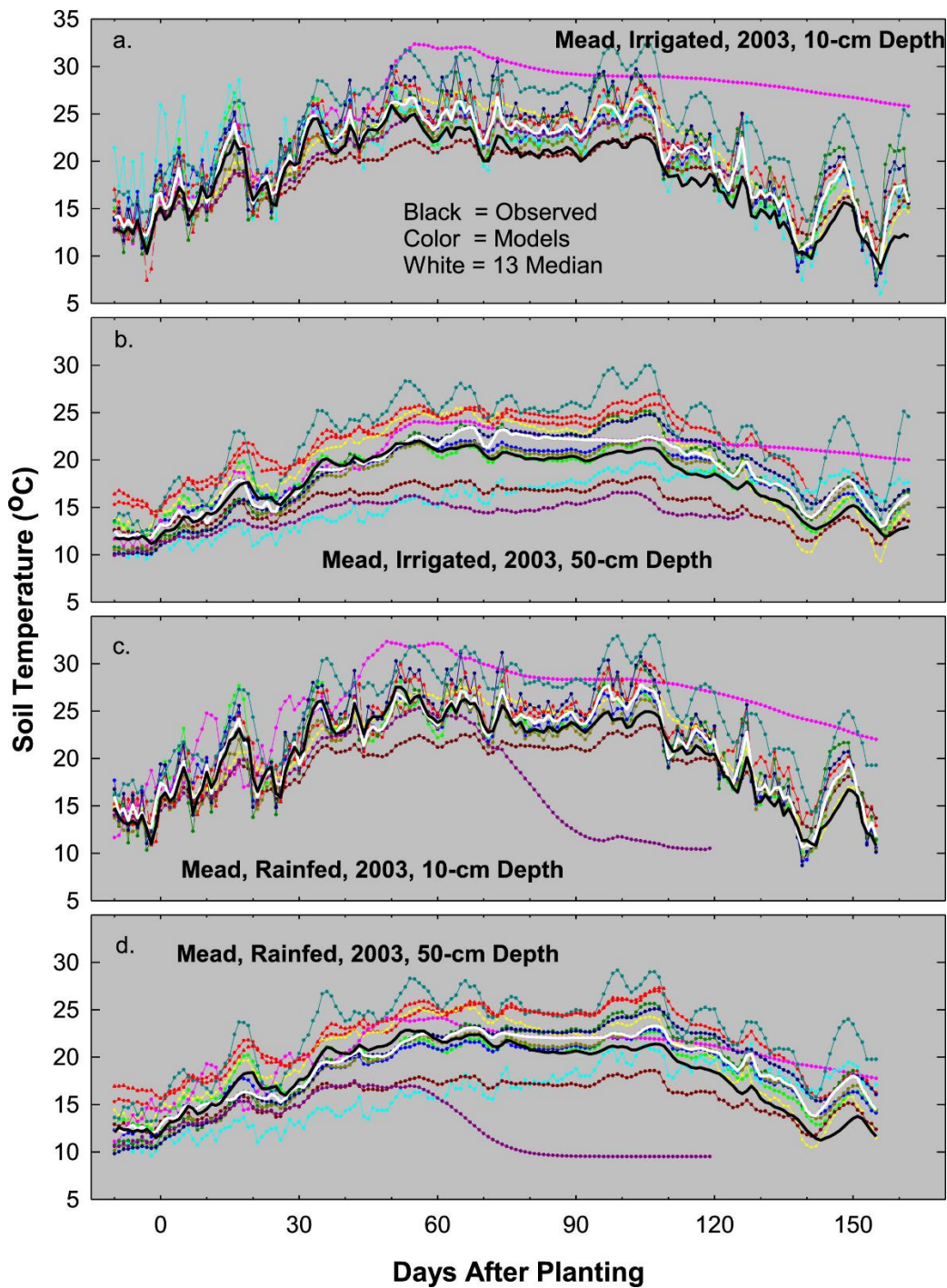


Figure 2. (a) Simulated soil temperatures from 13 families of maize growth models from the 10-cm depth in an irrigated field at Mead in 2003 along with the corresponding observed values. Also shown is the median of the 13 averaged-family curves. (b) Like “a” but for the 50-cm depth. (c). Like “a” but for a non-irrigated rainfed field. (d) Like “c” but for the 50-cm depth.



3.2. SOIL TEMPERATURES (ST) FOR 13 FAMILIES OF MAIZE GROWTH MODELS VERSUS DAYS AFTER PLANTING (DAP) FOR MEAD IN 2003 (DRIEST YEAR) AND FOR BUSHLAND WITH MESA IRRIGATION IN 2013 (YEAR WITH HIGHEST ET RATES)

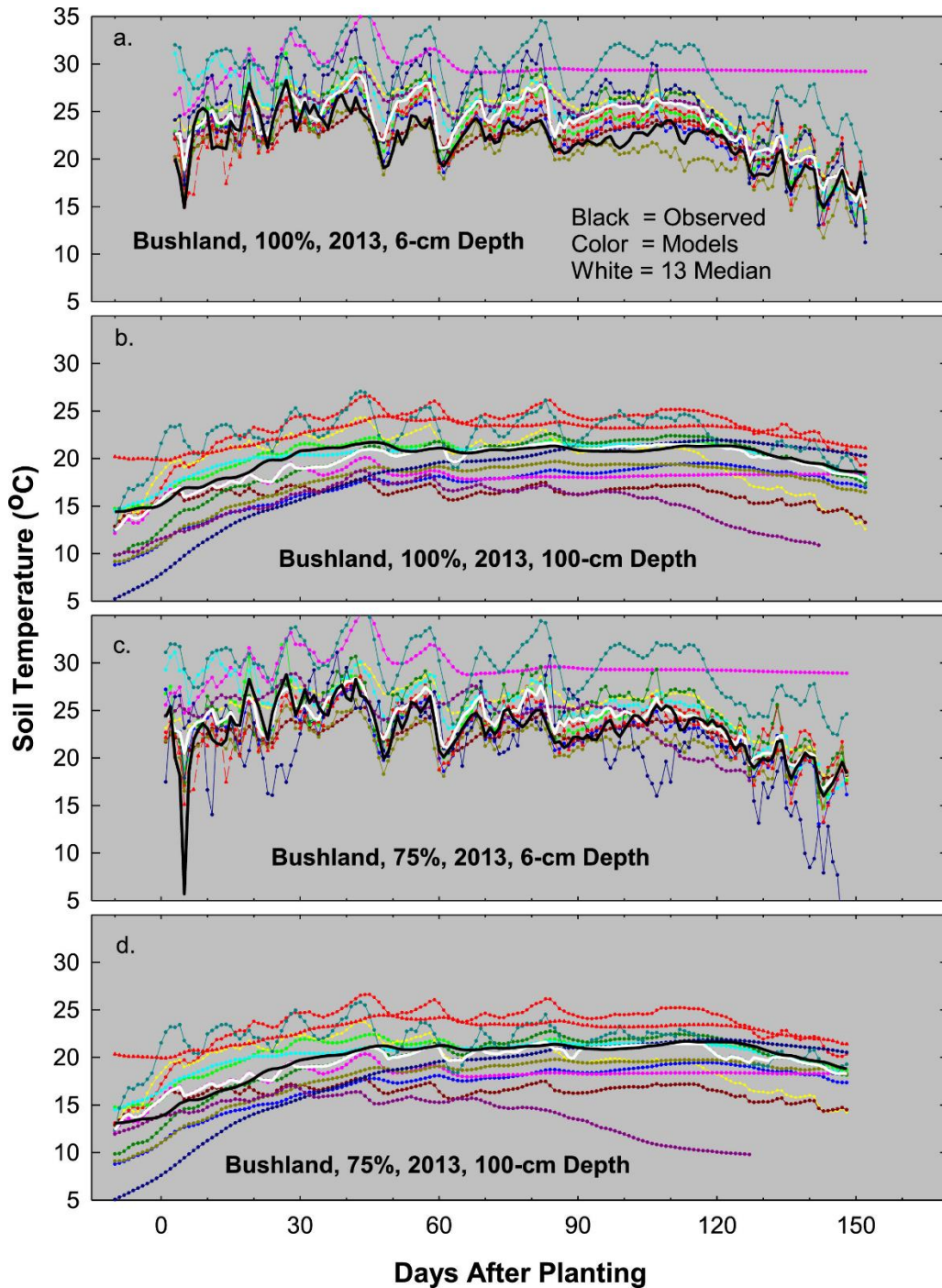
Most of the models tended to overestimate ST at the 10-cm depth in the irrigated field at Mead in 2003 (Figure 2a). One model (pink curve) seemed to really get off track about a third of the way through the season. The white curve is the median of the 13 families after the within-family averaging, and it is close to the observed curve early in the season, but it is 2-3 °C warmer than observed for about the last 2/3 of the season. However, the range from coldest to warmest model families was about 10 °C. In contrast, at the 50-cm depth (Figure 2b), the range among the model families is even wider (about 15 °C at midseason), yet the 13-family median curve is close to the observed curve.

For the Mead rainfed field at the 10-cm depth (Figure 2c), most of the family-averaged models were closer to the observed curve, as indicated by the white median. However, two models really went off track about a third and a half of the way through the season, but one was too warm (pink curve) and the other was too cold (purple curve). Focusing next on the 50-cm depth (Figure 2d), the too-cold curve was again too cold, but the warm one seemed to “behave” itself all season long. Ignoring the cold outlier, there still was about a 10 °C spread among the models, yet the 13-family median was close to the observed until about halfway through the season when it began to diverge and became about 3 °C warmer by the end of the season.

As happened at the 10-cm depth at Mead, most of the models simulated STs that were too warm at the 6-cm depth in Bushland (Figs. 3a,c), especially the field with 100 % MESA irrigation (Figure 3a). The field with 100 % MESA irrigation was the field with the largest evaporative loss, which would tend to cool the soil noticeably at shallow depth (Evelt et al., 2019). Again, there was a range of about 10 °C from coldest to warmest simulated ETs, and this was repeated for all four cases in Figure 3. At the 100-cm depths (Figs. 3b,d), there were about equal numbers of models that were too cold and too warm, and the 13-family median was close to the observations.

The down-plunging peak at DAP 5 in Figure 3c is interesting in that it indicates how much and how quickly bare, dry soil can change temperature at shallow depths. The down-plunging peak for 100 % irrigation (Figure 3a) did not change as much. In any event, apparently all the models have day-to-day running averages, and none followed this quick, cold weather change with their ST simulations.

Figure 3. Similar to Figure 2 except for the soil temperatures at the 6- and 100-cm depths of fields at Bushland that were irrigated to supply 100 % or 75 % replacement of soil moisture in 2013.



3.3. RANKING OF MODEL FAMILIES WITH RESPECT TO THEIR ABILITY TO SIMULATE SOIL TEMPERATURES

The RMSE for all 33 models, all 20 treatment-years, and 2 depths were extracted from Supplementary Statistics and Graphs. Then, they were averaged within model families and results for the 13 families are shown for four data sets in Figure 4: Mead at 10- and 50-cm depths and Bushland at 6- and 100-cm depths. Finally, they were ranked according to lowest RMSE among the family groups with the best six being identified. For Mead at the 10-cm depth, ecosys was best followed by APSIM, Jules, SLFT, STICS, and Biome. The RMSE range from about 1.5 °C for ecosys to 7 °C for the worst, so the range was quite large. Moving to 50cm depth (Figure 4b), Jules, ecosys, APSIM, and SLFT were again among the best six, along with Expert-N and SALUS. The range was from about 1.1 °C for Jules to about 6.7 °C. Looking at the 6-cm depth for Bushland (Figure 4c) five of the models that were best in Mead at 10-cm (Figure 4a) were also best at this shallow depth in Bushland (Jules, APSIM, Biome, ecosys, and STICS) with MaizSim also entering the best six. The range was from 1.5 °C for Jules to 8.1 °C for the worst. At the 100-cm depth in Bushland (Figure 4d), again APSIM, Expert-N, SLFT, and ecosys were among the best six, joined by DayCent and ARMOSA. The range was from about 1.0 °C for DayCent to 5.9 °C for the worst. Tabulating across the 4 data sets, ecosys and APSIM appear in 4, Jules and SLFT appear in 3, STICS, Biome, and Expert-N appear in 2, and SALUS, MaizSim, DayCent, and ARMOSA appear in 1.

Most of the errors in the worst models were due to standard biases (SB, Figure 5). The best models in all four categories (two sites and two depths at each site) had almost no standard biases nor non-linearity errors. As already mentioned, the remaining lack-of-correlation errors could be due to scatter in the observed data and input parameters.

Extending from the four data sets in Figs. 4 and 5, the ranking of the 13 model families for all 20 treatment-years and all depths is shown in Figure 6. The best model-families with the lowest RMSE were APSIM, ecosys, Jules, Expert-N, SLFT, and MaizSim. Somewhat surprisingly, the smallest RMSE with APSIM at about 1.6 °C in Figure 6a was a little larger than the smallest ones in Figure 4, whereas the worst model at about 5.1 °C in Figure 6a is about 1 °C better than the worst ones in Figure 4. Similar to Figure 5, the worst models in Figure 6b have large standard biases, whereas the best ones have almost no standard biases nor non-linearity of their slopes. The lack-of-correlation errors were small and about the same for about the best eight models, again suggesting these errors could be due to scatter in the observed data or input parameters.

Figure 4. (a) Ranking of 13 maize model families according to their root mean square errors (RMSE) for simulating daily soil temperature at the 10-cm depth for the 12 treatments at Mead with the best six models identified by name. Because there were no significant differences among “flavors” of models within the DSSAT-CSM, STICS, Expert-N, and MaizSim families, averages were obtained across the flavors. (b) Same as “a” except for the 50-cm depth at Mead. (c) Same as “a” except for the 6-cm depth of the 8 treatments at Bushland. (d) Same as “c” except for the 100-cm depth at Bushland.

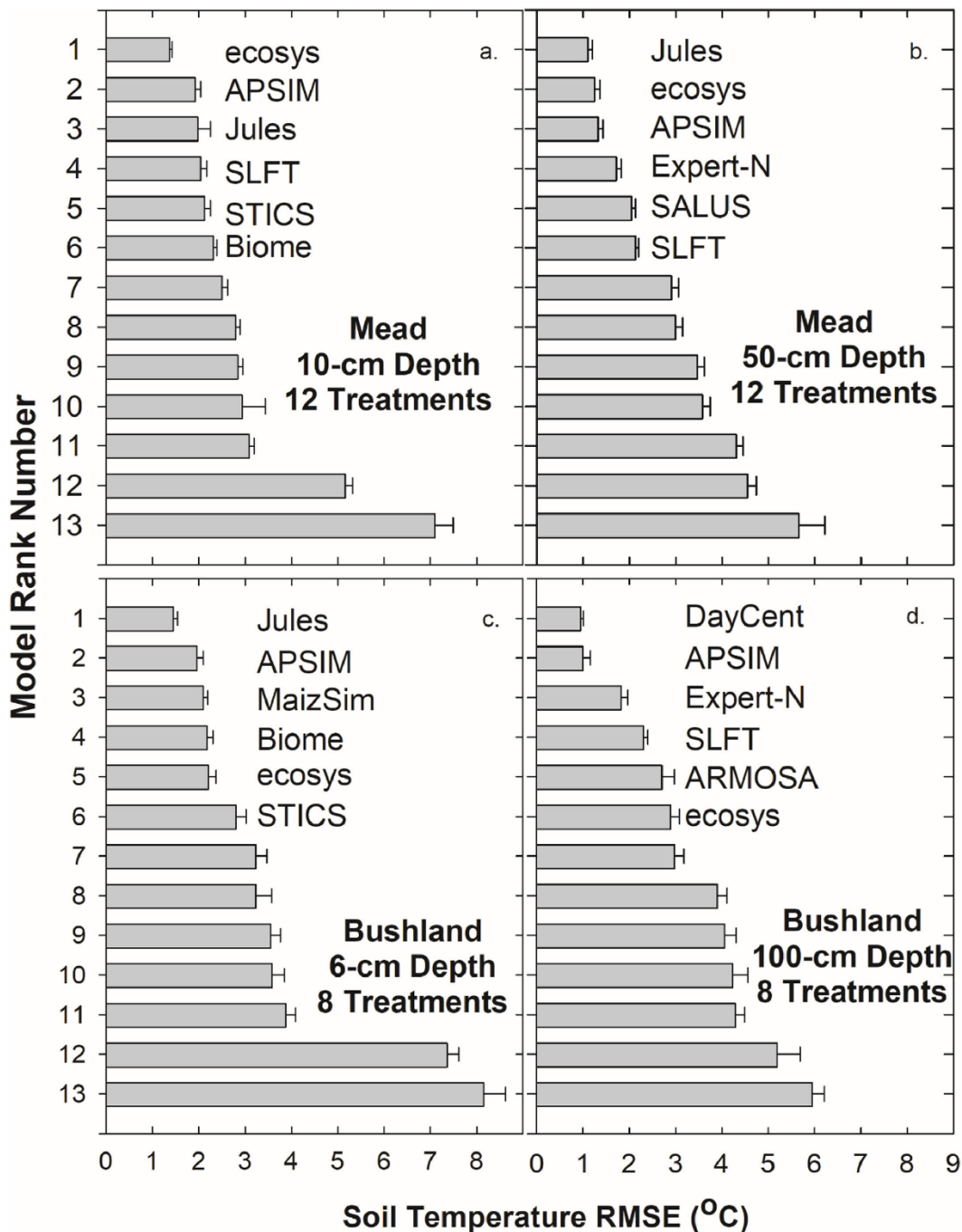
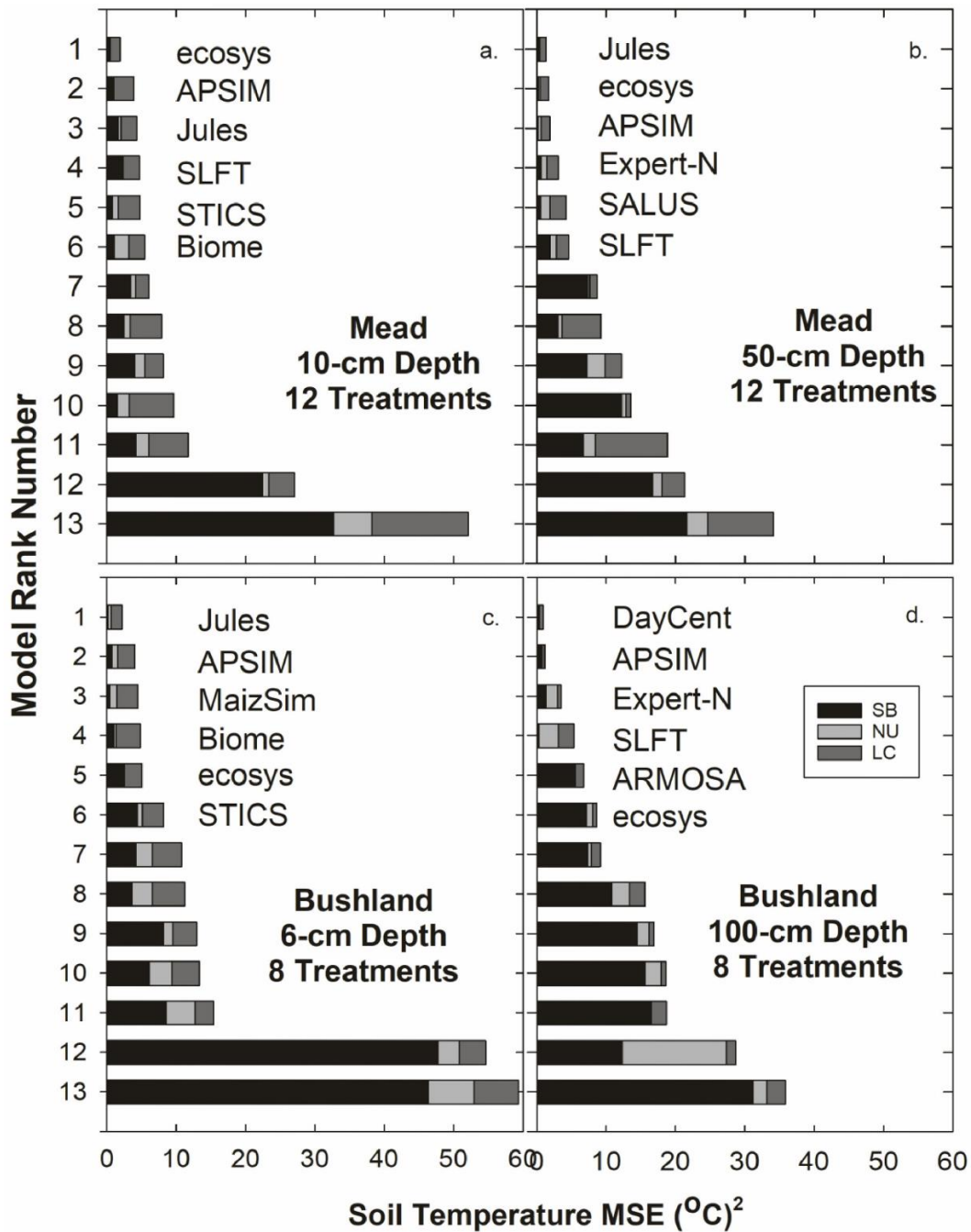


Figure 5. Similar to Figure 4 except that the mean square errors (MSE) are plotted as stacked bars following Gauch et al. (2003) to proportion the variances into standard biases (SB), non-linearity of the slopes (NL), and the lack of correlations (NC).



4. Discussion: numerical versus analytical methods for simulating soil temperature

Perusing Table S1, it appears that the modelers have followed two general approaches. One is the numerical method based on numerical, iterative solutions of the system of equations resulting from applying Eqs. (1) and 2 layer by layer from the top to the bottom of the rooted zone. APSIM, ecosys, Expert-N, Jules, and MaizSim all follow this approach, which essentially entails an energy balance on each layer, including the top layer. Simply put, the change in heat storage during a time step in each layer equals the difference between the heat flow into and that out of the layer. This approach results in a set of simultaneous equations which must be solved for the temperature of each layer. The temperature of the top layer for the numerical solution is determined by an energy balance at the soil surface among radiant, sensible, latent, and soil heat fluxes while the temperature of the bottom boundary must be specified. A problem is that to achieve good accuracy near the soil surface where the temperature gradient is often steep, the layers need to be thin. Then, to avoid numerical instability, one has to ensure that

$$\Delta t \leq 0.5C(\Delta z)^2 \kappa^{-1} \quad (\text{https://en.wikipedia.org/wiki/Von_Neu-mann_stability_analysis}).$$

This requirement led the developers of APSIM, for example, to impose 48 soil temperature time steps per “crop” time step for the rest of the model (Table S1). Of course, these extra time steps cost more computational time, but APSIM was the most accurate model in this inter-comparison (Figure 6), so the extra accuracy likely is worth the extra time. Five of the models using the numerical approach are among the most accurate six over all 20 treatment-years and two depths (Figure 6).

Among the five best models that used the numeric approach, as well as for those using the analytic approach, there could be several reasons why they differed in their accuracies to simulate soil temperature. The modelers could be using different algorithms to calculate soil heat capacity and/or thermal conductivity. The models also differ in their ability to simulate plant growth, transpiration, and soil water evaporation, all of which would result in differences in soil water content and consequent effects on soil heat capacity, thermal conductivity, and temperature. Different users also likely had differing skill in calibrating their models or also in the amount of effort they devoted to the task.

The other analytical approach being used by other models (ARMOSA, Biome, DSSAT-CSM (all flavors), L5SH, SALUS, SLFT, and STICS) involves variations of a damped annual sine wave (Eq. (4)). One big variation involves the annual amplitude, A . Several of the models, including the many DSSAT-CSM flavors, appear to follow the methods in EPIC (Williams et al., 1984, 1989) or APEX (Williams et al., 2005, 2008), which simulate A as half the difference between the average temperature of the hottest month minus that of the coldest month in the annual temperature cycle. Then they try to account for deviations from the annual cycle due to variations in weather patterns by adjustments to the average temperature for the particular day. However, the additions for all flavors of DSSAT-CSM included solar radiation terms which increased the soil surface temperatures above air temperature during daytime, but they appeared to ignore that soil temperatures are below

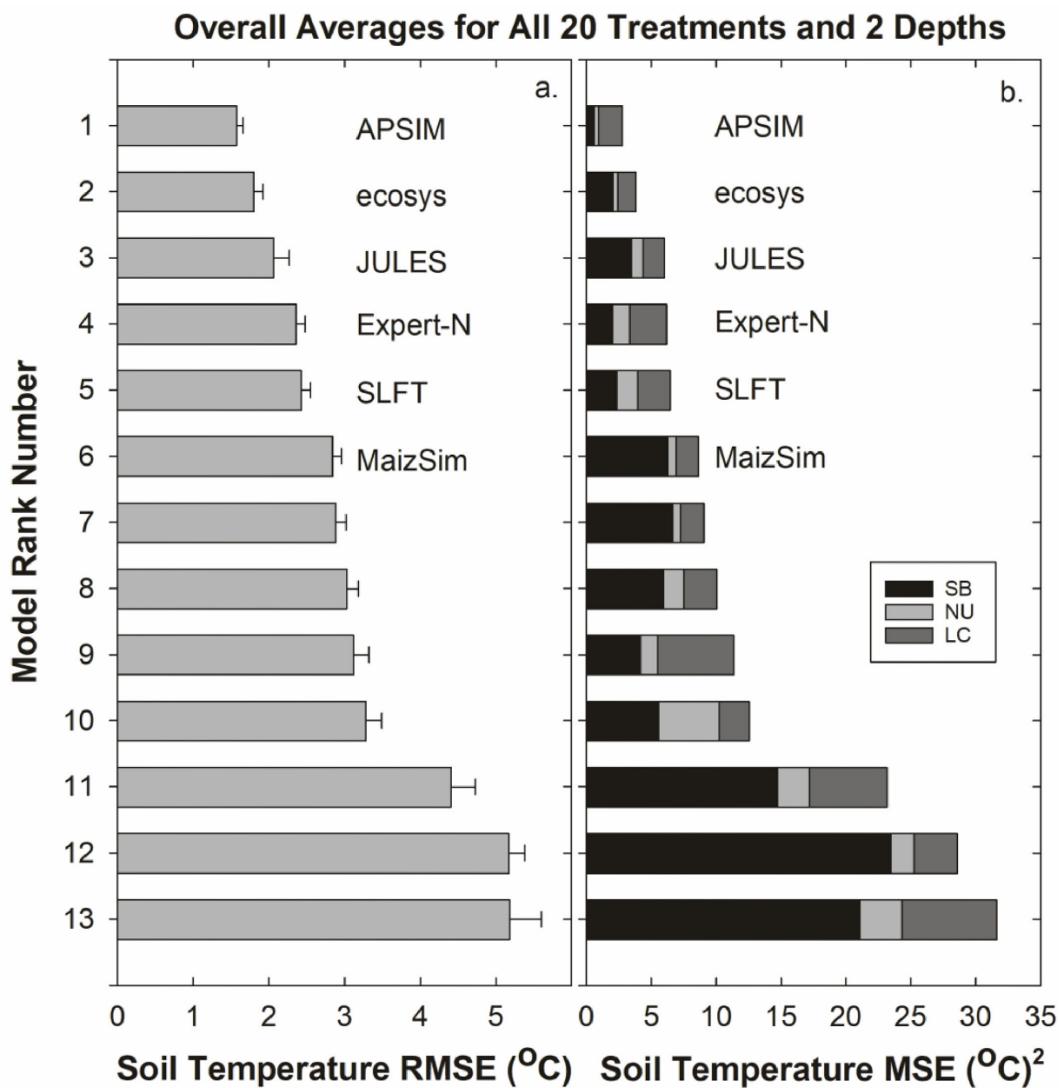
air temperature at night [as well as during the daytime for irrigated fields under arid conditions, e.g., Kimball et al. (2015)]. Consequently, all the flavors of DSSAT-CSM tended to overestimate soil temperatures in this study (Supplementary Statistics and Graphs). Indeed, changing the adjustment of A to using just the average air temperature for the previous five days with no radiation terms reduced the RMSE of soil temperature simulated by DSSAT-CSM to about 1/3 of that of the previous default equation, a change that will be implemented in the next version release (personal communication). EPIC (Williams et al., 1984, 1989) also has solar radiation terms, but it has some accounting for prior wet days, so it performs better than the default in DSSAT-CSM (personal communication). Two decades later, APEX (Williams et al., 2005, 2008) still has changes based on radiation in the adjustments to A, but now they are based on net radiation which appears to be negative until the net radiation exceeds $+14 \text{ MJ m}^{-2} \text{ d}^{-1}$. Those models that use a damped sine wave but do an energy balance on the top layer (i.e., STICS and SLFT) appeared to do better than those prescribing a certain portion of incident or net radiation. SLFT managed to be among the best six (Figure 6). Another likely source of error using Eq. (4) is that it presumes that the soil properties (constituents, bulk density, water content) are constant, so these are being averaged over the whole profile. However, applying Eq. (4) to a layered soil quickly becomes quite complex, as shown theoretically by van Wijk and Derksen (1963). A variant in use of Eq. (4) that could be explored is the application of it to successively deeper soil layers such that thermal conductivity and heat capacity could be recalculated for each layer according to the simulated water content of that layer. Although not theoretically correct, it would be constrained to go toward T_{avg} , so this approach could be more accurate than averaging soil properties over the whole profile. In any event, using an analytical equation like Eq. (4) enables soil temperature to be calculated quickly at any depth and time without any iterations or worry about numerical instability.

In any event, the large range of about 10-15 °C in simulated ST (Figs. 2, 3) from the coolest to warmest models all season long from bare soil to full canopy and at both shallow and deeper depths and at both locations is of concern. Such large differences in ST would affect many soil processes like decomposition, mineralization, and evaporation, as well as direct effects on plant growth, such as altering the time from germination to emergence. However, more important than the range among the models is whether any of the models are accurate compared to the measured STs. As presented earlier, the model family RMSEs averaged over all 20 treatment-years and 2 depths ranged from about 1.5 to 5.1 °C, so the best model family had errors that were less than a third of those of the worst, which should also improve the simulation of all the other soil and plant processes.

The lack of significant differences in the RMSE errors among the flavors of the DSSAT-CSM, STICS, Expert-N, and MaizSim in their simulations of ST are somewhat surprising considering that there were large changes in water content at various times during the seasons among the 20 treatment-years and that there were significant differences among the flavors in their ability to simulate evapotranspiration and soil water content (Kimball et al., 2023). However, although the heat capacity of water is about double that of quartz and other soil minerals, the thermal conductivities of quartz and other soil minerals are 15 and 5 times greater, respectively, than those of water (De Vries, 1963), so apparently the errors in ST simulation are more dominated by the accuracy of the

solid matter thermal conductivity simulation than the errors in evapotranspiration or soil water simulation.

Figure 6. (a.) Ranking of 13 maize model families according their root mean square errors (RMSE) for simulating daily soil temperature at the 10- and 50-cm depths at Mead and for the 6- and 100-cm depths at Bushland for all 20 treatment-years with the best six models identified by name. Because there were no significant differences in RMSE among “flavors” of models within the DSSAT-CSM, STICS, Expert-N, and MaizSim families, overall average RMSEs were calculated across the flavors. (b.) Similar to (a.) except that the mean square errors (MSE) are plotted as stacked bars following Gauch et al. (2003) to proportion the variances due to standard biases (SB), non-linearity of the slopes (NL), and the lack of correlations (NC).



5. Conclusions

- 5.1. Ignoring a couple of outliers, there was a range of about 10-15 °C from the coolest to warmest models all season long from bare soil to full canopy and at both shallow and deeper depths.
- 5.2. The model family RMSEs averaged over all 20 treatment-years and 2 depths ranged from about 1.5 to 5.1 °C.
- 5.3. Most of errors of the worst models were due to large standard biases, whereas the several best models had relatively small but similar lack-of-correlation errors, suggesting these errors could be due to scatter in the data. These best models had very little standard biases nor non-linearity of their slopes.
- 5.4. Within the DSSAT-CSM, STICS, Expert-N and MaizSim model families, there were no significant differences among the errors of their simulations of soil temperature due to their “flavor” methods for simulating evapotranspiration.
- 5.5. The six model families with the lowest RMSEs were APSIM, ecosys, JULES, Expert-N, SLFT, and MaizSim.
- 5.6. Five of these six best models (APSIM, ecosys, JULES, Expert-N, and MaizSim) used a numerical approach, which essentially entails an energy balance on each soil layer, including the soil surface, whereby the change in heat storage during a time step equals the difference between the heat flow into and that out of the layer.
- 5.7. Further improvements in even the best models for simulating soil temperature might be possible by incorporating more recent algorithms for simulating soil thermal conductivity.

CREDIT AUTHORSHIP CONTRIBUTION STATEMENT

Bruce A. Kimball: Conceptualization, Data curation, Formal analysis, Investigation, Methodology, Project administration, Validation, Visualization, Writing - original draft, Writing - review & editing. Kelly R. Thorp: Conceptualization, Data curation, Formal analysis, Investigation, Methodology, Validation, Visualization, Writing - review & editing. Kenneth J. Boote: Conceptualization, Data curation, Formal analysis, Investigation, Methodology, Project administration, Validation, Visualization, Writing - review & editing. Claudio Stockle: Conceptualization, Formal analysis, Methodology, Validation, Visualization, Writing - review & editing. Andrew E. Suyker: Conceptualization, Data curation, Formal analysis, Investigation, Methodology, Validation. Steven R. Evett: Conceptualization, Data curation, Formal analysis, Investigation, Methodology, Validation, Visualization, Writing - review & editing. David K. Brauer: Data curation, Formal analysis, Investigation, Methodology. Gwen G. Coyle: Data curation, Formal analysis, Investigation, Methodology. Karen S. Copeland: Data curation, Formal analysis, Investigation, Methodology. Gary W. Marek: Data curation, Formal analysis, Investigation, Methodology. Paul D. Colaizzi: Data curation, Formal analysis, Investigation, Methodology. Marco Acutis: Conceptualization, Data curation, Formal analysis, Investigation, Methodology, Writing - review & editing, Software. Sotirios Archontoulis: Conceptualization, Data curation, Formal analysis, Investigation, Methodology, Validation, Writing - review & editing, Software. Faye Babacar: Conceptualization, Data curation, Formal analysis, Investigation, Methodology, Software. Zoltan Barcza: Conceptualization, Data curation, Formal analysis, Investigation, Methodology, Software, Writing - review & editing. Bruno Basso: Conceptualization, Data curation, Formal analysis, Investigation, Methodology, Software, Writing - review & editing. Patrick Bertuzzi: Conceptualization, Data curation, Formal analysis, Investigation, Methodology, Software. Massimiliano De Antoni Migliorati: Conceptualization, Data curation, Formal analysis, Investigation, Methodology, Software, Writing - review & editing. Benjamin Dumont: Conceptualization, Data curation, Formal analysis, Investigation, Methodology, Software. Jean-Louis Durand: Conceptualization, Formal analysis, Investigation, Methodology, Writing - review & editing. Nándor Fodor: Conceptualization, Data curation, Formal analysis, Investigation, Methodology, Software. Thomas Gaiser: Conceptualization, Data curation, Formal analysis, Investigation, Methodology, Software, Writing - review & editing. Sebastian Gayler: Conceptualization, Data curation, Formal analysis, Investigation, Methodology, Software. Robert Grant: Conceptualization, Data curation, Formal analysis, Investigation, Methodology, Software. Kaiyu Guan: Conceptualization, Data curation, Formal analysis, Investigation, Methodology, Software. Gerrit Hoogenboom: Conceptualization, Data curation, Formal analysis, Funding acquisition, Investigation, Methodology, Software, Supervision, Writing - review & editing. Qianjing Jiang: Conceptualization, Data curation, Formal analysis, Investigation, Methodology, Software. Soo-Hyung Kim: Conceptualization, Data curation, Formal analysis, Investigation, Methodology, Software, Writing - review & editing. Isaya Kisekka: Conceptualization, Data curation, Formal analysis, Investigation, Methodology, Software. Jon Lizaso: Conceptualization, Data curation, Formal analysis, Investigation, Software, Writing - review & editing. Alessia Perego: Conceptualization, Data curation, Formal analysis, Investigation, Methodology, Software. Bin Peng: Conceptualization, Data curation, Formal analysis, Investigation, Methodology, Software. Eckart Priesack: Conceptualization, Data curation, Formal analysis, Investigation, Methodology, Software. Zhiming Qi: Conceptualization, Data curation, Formal analysis, Methodology, Software, Investigation. Vakhtang Shelia: Conceptualization, Data curation, Formal analysis, Investigation, Methodology, Software. Amit Kumar Srivastava: Conceptualization, Data curation, Formal analysis, Investigation, Methodology, Software. Dennis Timlin: Conceptualization, Data curation, Formal analysis, Investigation, Methodology, Software, Writing - review & editing. Heidi Webber: Conceptualization, Data curation, Formal analysis, Investigation, Methodology. Tobias Weber: Conceptualization, Data curation, Formal analysis, Investigation, Methodology, Software. Karina Williams: Conceptualization, Data curation, Formal analysis, Investigation, Software. Michelle Viswanathan: Conceptualization, Data curation, Formal analysis, Investigation, Methodology, Software. Wang Zhou: Conceptualization, Data curation, Formal analysis, Investigation, Methodology, Software.

ACKNOWLEDGEMENTS

We appreciate access to the comprehensive dataset from Mead, Nebraska, USA, which was collected by the following scientists: Shashi B. Verma, Achim Dobermann, Kenneth G. Cassman, Daniel T. Walters, Johannes M. Knops, Timothy J. Arkebauer, George G. Burba, Brigid Amos, Haishum Yang, Daniel Ginting, Kenneth G. Hubbard, Anatoly A. Gitelson, and Elizabeth A. Walter-Shea. The dataset was collected with support from the DOE-Office of Science (BER: Grant Nos. DE- FG03-00ER62996 and DE-FG02-03ER63639), DOE-EPSCoR (Grant No. DE-FG02-00ER45827), and the Cooperative State Research, Education, and Extension Service, US Department of Agriculture (Agreement No.2001-38700-11092). Funding was also provided by the National Multidisciplinary Laboratory for Climate Change, RRF- 2.3.1-21-2022-00014 project. Additional support was provided by grant "Advanced research supporting the forestry and wood-processing sector's adaptation to global change and the 4th industrial revolution", No. CZ.02.1.01/0.0/0.0/16_019/0000803 financed by OP RDE. The Nebraska sites were also supported by a subaward as part of the AmeriFlux Management Project from the University of California- Berkeley National Lab (Prime Sponsor: Department of Energy) and the Nebraska Agricultural Experiment Station with funding from the Hatch Act (Accession Number 1002649) through the USDA National Institute of Food and Agriculture. The dataset from Bushland, Texas, USA was acquired with support from the Ogallala Aquifer Program, a consortium between USDA-Agricultural Research Service, Kansas State University, Texas AgriLife Research, Texas AgriLife Extension Service, Texas Tech University, and West Texas A&M University. KW was supported by the Met Office Hadley Centre Climate Programme funded by BEIS.

SUPPLEMENTARY MATERIALS

Supplementary material associated with this article can be found, in the online version, at [doi:10.1016/j.agrformet.2024.110003](https://doi.org/10.1016/j.agrformet.2024.110003).

References

Allen, R.G., Pereira, L.S., Raes, D., Smith, M., 1998. Crop Evapotranspiration: Guidelines for Computing Crop Water Requirements, FAO Irrigation and Drainage Paper 56. Food and Agriculture Organization of the United Nations, Rome, Italy.

Allen, R.G., Walter, I.A., Elliott, R., Howell, T., Itenfisu, D., Jensen, M., Snyder, R.L., 2005. The ASCE Standardized Reference Evapotranspiration Equation. American Society of Civil Engineers, Reston, Virginia, p. 195.

Archontoulis, S., Miguez, F.E., Moore, K.J., 2014. Evaluating APSIM Maize, soil water, soil nitrogen, manure, and soil temperature modules in the Midwestern United States. *Agron J* 106 (3), 1025–1040.

Basso, B., Ritchie, J.T., 2015. Simulating crop growth and biogeochemical fluxes in response to land management using the SALUS model. G.P.. In: Hamilton, S.K., Doll, J.E., Robertson, G.P. (Eds.), *The Ecology of Agricultural Landscapes: LongTerm Research On the Path to Sustainability*. Oxford University Press, New York, New York, USA, pp. 252–274.

Best, M.J., Pryor, M., Clark, D.B., Rooney, G.G., Essery, Menard, C.B., Edwards, J.M., Hendry, M.A., Porson, A., Gedney, A.N., Mercado, L.M., Sitch, S., Blyth, E., Boucher, O., Cox, P.M., Grimmond, C.S.B., 2011. The joint UK land environment simulator (JULES), model description Part 1: energy and water fluxes. *Geoscient. Model Develop.* 4 (3), 677–699. <https://doi.org/10.5194/gmd-4-677-2011>, 01 September 2011.

Black, T.A., Thurtell, G.W., Tanner, C.B., 1968. Hydraulic load cell lysimeter, construction, calibration, and tests. *Soil Sci. Soc. Am. Proceed.* 32 (5), 623–629. <https://doi.org/10.2136/sssaj1968.03615995003200050016x>.

Brisson, N., Gary, C., Justes, E., Roche, R., Mary, B., Ripoche, D., Zimmer, D., Sierra, J., Bertuzzi, P., Burger, P., Bussiere, F., Cabidoche, Y.M., Cellier, P., Debaeke, P., Gaudillere, J.P., Henault, C., Maraux, F., Sequin, B., Sinoquet, H., 2003. An overview of crop model STICS. *Eur. J. Agron.* 18, 309–332.

Campbell, G.S., 1977. *An Introduction to Environmental Physics*. Springer Verlag, New York, New York, p. 159.

Campbell, G.S., 1985. *Soil Physics with BASIC*. Elsevier, Amsterdam.

Campbell, G.S., Jungbauer Jr., J.D., Bidlake, W.R., Hungerford, R.D., 1994. Predicting the effect of temperature on soil thermal conductivity. *Soil Sci* 158 (5), 307–313.

Côte, J., Konrad, J.-M., 2005. A generalized thermal conductivity model for soils and construction materials. *Canad. Geotech. J.* 42, 443–458. <https://doi.org/10.1139/T04-106>.

DeJonge, K.C., Thorp, K.R., 2017. Standardized reference evapotranspiration and dual crop coefficient approach in the DSSAT cropping system model. *Trans. ASABE* 60 (6), 1965–1981.

De Vries, D.A., 1963. Thermal properties of soils. In: van Wijk, W.R. (Ed.), *Physics of Plant Environment*. John Wiley & Sons, Inc., New York, pp. 210–235.

Dugas, W.A., Bland, W.L., 1991. Springtime soil temperatures in lysimeters in central Texas. *Soil Sci* 152 (2), 87–91.

Evet, S.R., Agam, N., Kustas, W.P., Colaizzi, P.D., Schwartz, R.C., 2012. Soil profile method for soil thermal diffusivity, conductivity and heat flux: comparison to soil heat flux plates. *Adv. Water Resour.* 50 (2012), 41–54.

Evet, S.R., Marek, G.W., Colaizzi, P.D., Brauer, D.K., O’Shaughnessy, S.A., 2019. Corn and sorghum ET, E, yield, and CWP as affected by irrigation application method: SDI versus mid-elevation spray irrigation. *Transact. ASABE* 62 (5), 1377–1393. <https://doi.org/10.13031/trans.13314>.

Evet, S.R., Marek, G.W., Colaizzi, P.D., Brauer, D.K., Howell, T.A., 2020. Are crop coefficients for SDI different from those for sprinkler irrigation application? *Transact. ASABE* 63 (5), 1233–1242. <https://doi.org/10.13031/trans.13920>.

- Evet, S.R., Copeland, K.S., Ruthardt, B.B., Marek, G.W., Colaizzi, P.D., Howell Sr., T.A., Brauer, D.K., 2022. The Bushland, Texas maize for grain datasets. *Ag. Data Commons*. <https://doi.org/10.15482/USDA.ADC/1526317>.
- Gauch, H.G., Hwang, J.T.G., Fick, G.W., 2003. Model evaluation by comparison of model-based predictions and measured values. *Agron. J.* 95, 1442–1446.
- Grant, R.F., Flanagan, L.B., 2007. Modeling stomatal and nonstomatal effects of water deficits on CO₂ fixation in a semiarid grassland. *J. Geophys. Res.* 112, G03011. <https://doi.org/10.1029/2006JG000302>.
- Hidy, D., Barcza, Z., Marjanovic, H., Ostrogovic Sever, M.Z., Dobor, L., Gelybo, G., Fodor, N., Pinter, K., Churkina, G., Running, S., Thornton, P., Bellocchi, G., Haszpra, L., Horvath, F., Suyker, A., Nagy, Z., 2016. Terrestrial Ecosystem Process Model Biome-BGCMuSo v4.0: summary of improvements and new modeling possibilities. *Geoscient. Model Develop.* 9, 4405–4437. <https://doi.org/10.5194/gmd-9-4405-2016>.
- Hoffmann, F., Beinhauer, R., Dadoun, F., 1993. Soil temperature model for CERES and similar crop models. *J. Agronomy Crop Sci.* 170, 56–63.
- Hoogenboom, G., Porter, C.H., Boote, K.J., Shelia, V., Wilkens, P.W., Singh, U., White, J. W., Asseng, S., Lizaso, J.I., Moreno, L.P., Pavan, W., Ogoshi, R., Hunt, L.A., Tsuji, G. Y., Jones, J.W., 2019a. The DSSAT crop modeling ecosystem. In: Boote, K. (Ed.), *Advances in Crop Modelling For a Sustainable Agriculture*. Burleigh Dodds Science Publishing, Cambridge, UK. ISBN: 978 1 78676 240 5. www.bdspublishing.com.
- Hoogenboom, G., Porter, C.H., Shelia, V., Boote, K.J., Singh, U., White, J.W., Hunt, L.A., Ogoshi, R., Lizaso, J.I., Koo, J., Asseng, S., Singles, A., Moreno, L.P., Jones, J.W., 2019b. Decision Support System For Agrotechnology Transfer (DSSAT) Version 4.7. DSSAT Foundation, Prosser, Washington. <http://dssat.net>.
- Johansen, O., 1975. Thermal Conductivity of Soils. University of Trondheim, Trondheim, Norway. Ph.D. thesis U.S. Army Corps of Engineers, Cold Regions Research and Engineering Laboratory, Hanover, New Hampshire. CRREL Draft English Translation 637.
- Jones, J.W., Hoogenboom, G., Porter, C.H., Boote, K.J., Batchelor, W.D., Hunt, L.A., Wilkens, P.W., Singh, U., Gijssman, A.J., Ritchie, J.T., 2003. The DSSAT cropping system model. *European J. Agron.* 18 (3–4), 235–265. [https://doi.org/10.1016/S1161-0301\(02\)00107-7](https://doi.org/10.1016/S1161-0301(02)00107-7).
- Keating, B.A., Carberry, P.S., Hammer, G.L., Probert, M.E., Robertson, M.J., Holzworth, D., Huth, N.I., Hargreaves, J.N.G., Meinke, H., Hochman, Z., McLean, G., Verburg, K., Snow, V., Dimes, J.P., Silburn, M., Wang, E., Brown, S., Bristow, K.L., Asseng, S., Chapman, S., McCown, R.L., Freebairn, D.M., Smith, C.J., 2003. An overview of APSIM, a model designed for farming system simulation. *Europ. J. Agron.* 18, 267–288.
- Kim, S.-H., Yang, Y., Timlin, D., Fleisher, D., Dathe, A., Reddy, V.R., Staver, K., 2012. Modeling temperature responses of leaf growth, development, and biomass in maize with MAIZSIM. *Agron J* 104, 1523–1537.
- Kimball, B.A., Jackson, R.D., Reginato, R.J., Nakayama, F.S., Idso, S.B., 1976. Comparison of field-measured and calculated soil-heat fluxes. *Soil Sci. Soc. Am. J.* 40 (1), 18–25.
- Kimball, B.A., Bellamy, L.A., 1986. Generation of diurnal solar radiation, temperature, and humidity patterns. *Ener. Agricult.* 5, 185–197.
- Kimball, B.A., White, J.W., Ottman, M.J., Wall, G.W., Bernacchi, C.J., Morgan, J., Smith, D.P., 2015. Predicting canopy temperatures and infrared heater energy requirements for warming field plots. *Agron J* 107, 129–141.
- Kimball, B.A., Thorp, K.R., Boote, K.J., Stockle, C., Suyker, A.E., Evett, S.R., Brauer, D.K., Coyle, G.G., Copeland, K.S., Marek, G.W., Colaizzi, P.D., Acutis, M., Alimaghani, S., Archontoulis, S., Babacar, F., Barcza, Z., Basso, B., Bertuzzi, P., Constantin, J., De Antoni Migliorati, M., Dumont, B., Durand, J.-L., Fodor, N., Gaiser, T., Garofalo, P., Gayler, S., Giglio, L., Grant, R., Guan, K., Hoogenboom, G., Jiang, Q., Kim, S.-H., Kisekka, I., Lizaso, J., Masia, S., Meng, H., Mereu, V., Mukhtar, A., Perego, A., Peng, B., Priesack, E., Qi, Z., Shelia, V., Snyder, R., Soltani, A., Spano, D., Srivastava, A.,

Thomson, A., Timlin, D., Trabucco, A., Webber, H., Weber, T., Willaume, M., Williams, K., van der Laan, M., Ventrella, D., Viswanathan, M., Xu, X., Zhou, W., 2023. Simulation of evapotranspiration and yield of maize: an intercomparison among 41 maize models. *Agric. For. Meteorol.* 333, 109396 <https://doi.org/10.1016/j.agrformet.2023.109396>.

Lu, S., Ren, T., Gong, Y., Horton, R., 2007. An improved model for predicting soil thermal conductivity from water content at room temperature. *Soil Sci. Soc. Am. J.* 71, 8–14.

Mahdavi, S.M., Neyshabouri, M.R., Fujimaki, H., 2016. Assessment of some soil thermal conductivity models via variations in temperature and bulk density a low moisture content. *Euras. Soil Sci.* 49 (8), 915–925. <https://doi.org/10.1134/S1064229316080068>.

McInnes, K.J., Kanemasu, E.T., Kissel, D.E., Sisson, J.B., 1986. Predicting diurnal variations in water content along with temperature at the soil surface. *Agric. For. Meteorol.* 38, 337–348.

Moore, C., Berardi, D., Blanc-Betes, E., DeLucia, E.H., Dracup, E.C., Egenriether, S., Gomez-Casanovas, S.N., Hartman, M.D., Hudiburg, T., Kantola, I., Masters, M.D., Parton, W.J., van Allen, R., von Haden, A.C., Wang, W.H., Bernacchi, C.J., 2020. The carbon and nitrogen cycle impacts of reverting perennial bioenergy switchgrass to an annual maize crop rotation. *GCB Bioener.* 12, 941–954. <https://doi.org/10.1111/gcbb.12743>.

Nobre, R.C.M., Thomson, N.R., 1993. The effects of transient temperature gradients on soil moisture dynamics. *J. Hydrol. (Amst)* 157, 57–101.

Parton, W.J., Logan, J.A., 1981. A model for diurnal variation in soil and air temperature. *Agricult. Meteorol.* 23, 205–216.

Perego, A., Giussani, A., Sanna, M., Fumagalli, M., Carozzi, M., Alfieri, L., Brenna, S., Acutis, M., 2013. The ARMOSA simulation crop model: overall features, calibration and validation results. *Ital. J. Agrometeorol.* 3, 23–38.

Priesack, E., Gayler, S., Hartmann, H.P., 2006. The impact of crop growth sub-model choice on simulated water and nitrogen balances. *Nutrient Cycl. Agroecosys.* 75, 1-13. <https://doi.org/10.1007/s10705-006-9006-1>.

Priestley, C.H.B., Taylor, R.J., 1972. On the assessment of surface heat flux and evaporation using large-scale parameters. *Monthly Weather Rev* 100, 81-92.

Ritchie, J.T., 1972. Model for predicting evaporation from a row crop with incomplete cover. *Water Resour. Res.* 8, 1204-1213.

Sandor, R., Barcza, Z., Hidy, D., Lellei-Kovacs, E., Ma, S., Bellocchi, G., 2016. Modelling of grassland fluxes in Europe: evaluation of two biogeochemical models. *Agricul., Ecosys. Environ.*, 215, 1-19. <https://doi.org/10.1016/Zi.agee.2015.09.001>.

Sandor, R., Barcza, Z., Acutis, M., Doro, L., Hidy, D., Kochy, M., Minet, J., Lellei-Kovacs, E., Ma, S., Perego, A., Rolinski, S., Ruget, F., Sanna, M., Seddaiu, G., Wu, L., Bellocchi, G., 2017. Multi-model simulation of soil temperature, soil water content and biomass in Euro-Mediterranean grasslands: uncertainties and ensemble performance. *European J. Agron.* 88, 22-40. <https://doi.org/10.1016/Zj.eja.2016.06.006>.

Sau, F., Boote, K.J., Bostick, W.M., Jones, J.W., Minguez, M.I., 2004. Testing and improving evapotranspiration and soil water balance of the DSSAT crop models. *Agron. J.* 96, 1243-1257.

Shelia, V., Simunek, J., Boote, K.J., Hoogenboom G, K.J., 2018. Coupling DSSAT and HYDRUS-1D for simulations of soil water dynamics in the soil-plant-atmosphere system. *J. Hydrol. Hydromech.* 66 (2), 232-245.

Simunek, J., Huang, K., van Genuchten, M., 1998. The HYDRUS Code For Simulating the one- dimensional movement of water, heat, and Multiple Solutes in Variably- Saturated media, Version 6.0., Tech. Rep. 144. U.S. Salinity Lab., United States Dep. of Agriculture, Agricultural Research Service.

- Simunek, J., van Genuchten, M.T., Sejna, M., 2008. Development and applications of the HYDRUS and STANMOD software packages and related codes. *Vadose Zone J.* 7 (2), 587. <https://doi.org/10.2136/vzj2007.0077>.
- Suleiman, A.A., Ritchie, J.T., 2003. Modeling soil water redistribution during second- stage evaporation. *Soil Sci. Soc. Amer. J.* 67, 377-386.
- Suleiman, A.A., Ritchie, J.T., 2004. Modifications to the DSSAT Vertical drainage model for more accurate soil water dynamics estimation. *Soil Sci* 169, 745-757. <https://doi.org/10.1097/01.ss.0000148740.90616.fd>.
- Suyker, A.E., Verma, S.B., Burba, G.G., Arkebauer, T.J., Walters, D.T., Hubbard, K.G., 2004. Growing season carbon dioxide exchange in irrigated and rainfed maize. *Agric. For. Meteorol.* 124, 1-13.
- Suyker, A.E., Verma, S.B., Burba, G.G., Arkebauer, T.J., 2005. Gross primary production and ecosystem respiration of irrigated maize and irrigated soybean during a growing season. *Agric. For. Meteorol.* 131, 180-190.
- Suyker, A.E., Verma, S.B., 2008. Interannual water vapor and energy exchange in an irrigated maize-based agroecosystem. *Agric. For. Meteorol.* 148, 417-427.
- Suyker, A.E., Verma, S.B., 2009. Evapotranspiration of irrigated and rainfed maize-soybean cropping systems. *Agric. For. Meteorol.* 149, 443-452.
- van Wijk, W.R., Derksen, W.J., 1963. Sinusoidal temperature variations in a layered soil. W.R. van Wijk *Physics of Plant Environment*. John Wiley & Sons, Inc., New York, pp. 171-209.
- van Wijk, W.R., De Vries, D.A., 1963. Periodic temperature variations in a homogeneous soil. W.R. van Wijk *Physics of Plant Environment*. John Wiley & Sons, Inc., New York, pp. 102-143.
- Williams, J.R., Jones, C.A., Dyke, P.T., 1984. A modelling approach to determining the relationship between erosion and soil productivity. *Transact. ASAE* 27, 129-144. <https://doi.org/10.13031/2013.32748>.
- Williams, J.R., Jones, C.A., Kiniry, J.R., Spanel, D.A., 1989. The EPIC crop growth model. *Transact. ASAE* 32 (2), 497-511.
- Williams, J.R., Izaurralde, C.A., 2005. Blackland Research Center Reports. In: *Blackland Research Center Reports*, 2. Blackland Research Center, USDA, Temple, TX, USA.
- Williams, J.R., Izaurralde, C.A., Steglich, E.M., 2008. Agricultural Policy/Environmental eXtender model. Theoretical Documentation Version 0604. AgriLIFE RESEARCH, Texas A&M System. BREC Report #2008-17.
- Willmott, C.J., 1982. Some comments on the evaluation of model performance. *Bullet. Am. Meteorol. Soc.* 63 (11), 1309-1313.
- Wolf, J., 2012. User Guide for LINTUL5: Simple Generic Model for Simulation of Crop Growth Under Potential, Water Limited and Nitrogen, Phosphorus and Potassium Limited Conditions. Wageningen University.